forests

MDPI

Article

Precipitation and Streamflow Reconstructions from Tree Rings for the Lower Kızılırmak River Basin, Turkey

Sena Genç and Hüseyin Tuncay Güner *

Forest Botany Department, Faculty of Forestry, Istanbul University-Cerrahpaşa, Bahçeköy, Istanbul 34473, Turkey; gencsna@gmail.com

* Correspondence: tuncay.guner@iuc.edu.tr

Abstract: The Kızılırmak River is the longest inland river, has the second-largest basin, and is one of the most important water sources of Turkey. On the other hand, flow data in the basin are too short-term and discordant, with too many gaps to provide reliable information regarding variations in river runoff. In this research, we reconstructed the April–July total precipitation and mean April–August streamflow of Gökırmak River at one gauge in the lower Kızılırmak River Basin using seven regional tree-ring chronologies. Tree-ring chronologies were highly correlated with the precipitation from April to July and with the streamflow from April to August. Both reconstructions successfully explained total variance in instrumental records with 0.36 (precipitation) and 0.35 (streamflow) R^2 values. We provided 210 years (1794–2003) of precipitation and streamflow reconstructions, which largely overlapped. Five extreme dry (1840, 1842, 1873, 1887, and 1947) and four extreme wet years (1829, 1837, 1814 and 1881) were determined. The longest consecutive drought and wet events were three years long, for the periods of 1926–1928 and 1835–1837, respectively. The 13-year low-pass filter values highlighted a 30-year-long (from 1843 to 1872) stationary period of April–August mean streamflow.

Keywords: dendrohydrology; *Pinus nigra*; drought; flood; Anatolia

Citation: Genç, S.; Güner, H.T. Precipitation and Streamflow Reconstructions from Tree Rings for the Lower Kızılırmak River Basin, Turkey. *Forests* **2022**, *13*, 501. https://doi.org/10.3390/f13040501

Academic Editor: Giovanna Battipaglia

Received: 8 February 2022
Accepted: 22 March 2022
Published: 23 March 2022

1. Introduction

Long, continuous, and reliable hydrological records are required to develop strategies for sustainable water management [1,2]; however, existing instrumental streamflow records are not sufficient to provide reliable information on decadal and centennial variations in river runoff [3]. Accordingly, the additional development of proxy data is needed from such sources as tree rings and lake sediments [2,4,5]. Annual rings from old trees in particular have been used widely to extend the instrumental meteorological data and hydroclimatic parameters to date back hundreds of years. In this way, a vast number of dendrohydrological studies have revealed the past climate [6–10] and flow regime of the prominent rivers used as water resources worldwide ([3,5,11–14] and many others). On the other hand, there are limited studies which date flash floods events [15,16].

The multi-century climate history of Turkey has been presented in tree-ring studies [8,17–22] for many regions. Although instrumental records of rivers barely date back to the 1950s in Turkey, there are only two studies focusing on streamflow reconstructions, which are in the Filyos River [4] and the Sakarya Basin [23]. The lack of studies on dendrohydrology in Turkey, which has been facing the negative effects of drought caused by climate change, encouraged us to conduct this research. Here, we particularly focused on the lower Kızılırmak River Basin (hereafter KRB), and presented streamflow and precipitation reconstructions for the basin. We designed our research in the KRB due to its strategic importance for water supply in Turkey. This importance comes from the fact that Kızılırmak River is the longest inland river and has the second-largest basin [24], approximately 11% of Turkey [25], which has 6.48 billion m^3 flow volume and it constitutes 3.5% of Turkey's

water potential [24]. In this research, we aimed (1) to build climate-sensitive black pine tree-ring chronologies, (2) to identify a climate–tree growth relationship and, finally, (3) to reconstruct streamflow as well as precipitation in lower KRB. We hypothesized that trees in old-growth black pine forests capture precipitation and, indirectly, streamflow signals due to the limiting effect of droughts; that will allow us to develop precipitation and streamflow reconstructions in the basin.

2. Materials and Methods

2.1. Study Area

KRB is located in the center of the Anatolian Peninsula and runs from Sivas to Samsun [26] (Figure 1). The main stem is 1151 km long and the total drainage basin is 78.180 km^2 [25]. The highest flow period was observed from March—which coincides with the snow starting to melt—to May (or June), and it reaches its highest level in April [26].

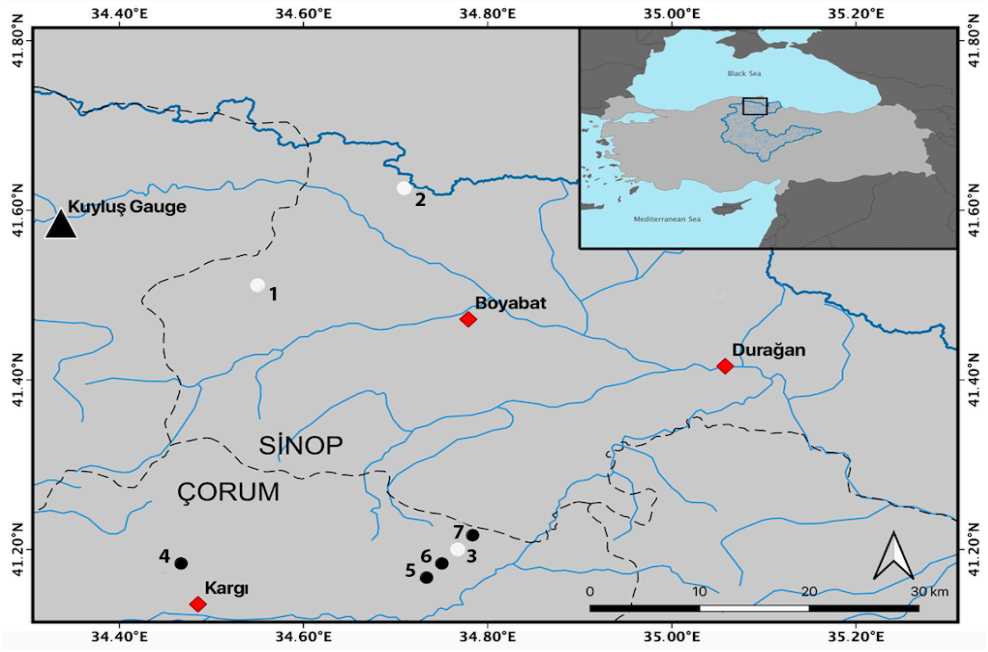

Figure 1. Tree-ring chronology sites in Kızılırmak River Basin. The white circles represent the newly sampled sites for this study (1 = HAC, 2 = MEM, 3 = BED), the black circles represent previously published chronologies (4 = KAR, [22]; 5 = IKI, (Akkemik et al. unpublished data); 6 = TIR, [4]; 7 = SAH, [22]) and the gray triangle represents the Kuyluş gauge on Kızılırmak River.

The annual mean precipitation in the KRB ranges from 300 to 800 mm and the mean annual temperature is 13.7 °C [24,27]. The continental climate with hot, dry summers and cold, snowy winters is dominant, since a large part of the KRB (upper and middle basin) is located on the Central Anatolian Plateau surrounded by the mountains. On the other hand, the lower basin where our research is conducted is mostly influenced by the milder and wetter Black Sea climate [26].

Although the KRB is the second-largest basin (land area), it is one of the basins with the lowest amount of forested area (19%) [28]. The KRB consists of Euro-Siberia and Iran-Turanian floristic regions shaped under the Black Sea and continental climates, respectively. Our research area is located in the lower KRB mostly characterized by the Euro-Siberia floristic region. The higher plateaus and mountains behind the Black Sea are covered by cold, sub-humid coniferous forests (*Abies nordmanniana* subsp. *equi-trojani* (Asch. and Sint. ex Boiss.) Coode and Cullen, *Pinus nigra* JF Arnold, and *Pinus sylvestris* L.), while lower elevations are mostly dominated by temperate broadleaf deciduous forests including *Fagus* L., *Alnus* Mill., and *Quercus* L. taxa [26,29].

2.2. Tree-Ring Data

We used seven black pine (*Pinus nigra* JF Arnold) chronologies in the lower KRB, four (KAR, IKI, SAH, and TIR) developed by previous studies ([4,22]; Akkemik et al. unpublished data) and three (HAC, MEM, and BED) newly developed for this study (Figure 1, Table 1). Two cores per tree were taken using the Haglöf increment borer. The collected samples were mounted and glued into the wooden channels based on following the standard dendrochronological techniques [30,31].

Table 1. The site characteristics and the details of the tree-ring chronology data used in the study.

Region	Site	Trees/Cores	Tree Species	Aspect	Elevation (m)	Lat (N)	Lon (E)	References
Sinop, Boyabat	HAC	15/30	PINI	SE	1179	41°30′	34°33′	This study
Sinop, Boyabat	MEM	5/10	PINI	SE	1334	41°37′	34°42′	This study
Çorum, Kargı	BED	12/24	PINI	SE	1233	41°12′	34°46′	This study
Çorum, Kargı	KAR	22/38	PINI	SW	1522	41°11′	34°28′	[22]
Çorum, Kargı	IKI	12/24	PINI	E	1156	41°10′	34°44′	Akkemik et al. unpublished data
Çorum, Kargı	TIR	32/64	PINI	NE	1428	41°11′	34°45′	[4]
Çorum, Kargı	SAH	17/34	PINI	S	1300	41°13′	34°47′	[22]

Tree-ring widths were measured with a precision of 0.001 mm using the LINTAB-TSAP measuring system (Rinntech, Germany) and the accuracy of the measurements was statistically confirmed using COFECHA [32,33]. We standardized the tree-ring measurement series by fitting a 67% cubic smoothing spline with a 50% cutoff frequency to remove non-climatic trends [34,35]. Then, chronologies were pre-whitened with low-order autoregressive models [36]. The biweight robust mean was used to obtain residual site chronologies. The minimum sample depth for each chronology was determined according to the expressed population signal (EPS; predetermined cut-off value is 0.85) [37,38]. In addition, we calculated mean sensitivity (MS), the mean inter-series correlation between all series, and signal-to-noise ratio (SNR) of residual chronologies to check the quality and reliability of the tree-ring chronologies. All these analyses were performed using the ARSTAN program [34].

2.3. Streamflow and Climate Data

We used CRU TS4.04 gridded at a resolution of 0.5° × 0.5° for monthly total precipitation and mean temperature datasets from the KNMI Climate Explorer [39] for the grid-covering tree-ring sites and streamflow gauge in the lower KRB (41°0′–41°30″ N, 34°30′–35°0′ E). We selected the period of 1930–2003, which maximizes the meteorological stations' recording period in the area. The climatic diagram of lower KRB shows that the basin receives higher precipitation from December to June (reaches the highest value in May) and lowest from July to September (reaches the lowest value in August). The highest mean temperatures were observed during the months of July and August (Figure 2).

In addition, monthly streamflow data for the gauges within KRB were obtained from the General Directorate of Electrical Power Resources, Survey and Development Administration (EIEI). Although the EIEI streamflow-gauging program started collecting streamflow data in 1935, very few gauge stations go back as early as 1935 [23]. Despite the presence of 49 gauges in the KRB, most of the data have short-term and discordant records with a high number of gaps. Between these gauges, Gökırmak-Kuyluş (1954–1998) was chosen for this study because it provides relatively longer records and gives statistically significant correlations with the tree-ring data. Weka machine learning software [40], an open source program, was used to estimate missing monthly streamflow data of the station for the years 1954, 1957, 1961, and 1962.

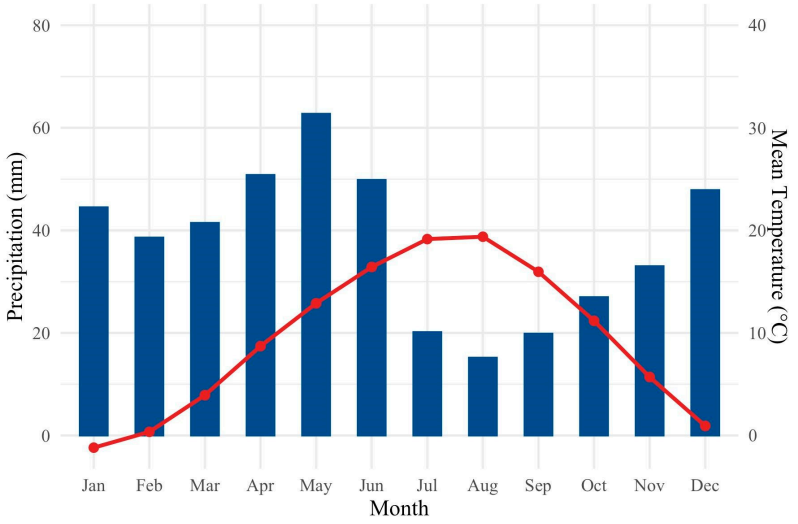

Figure 2. The lower KRB basin climatic diagram. It was drawn using the CRU TS4.04 monthly total precipitation and mean temperature data of the lower KRB. Red line and bars represent mean temperature (°C) and precipitation (mm), respectively.

According to the monthly hydrogram of Kuyluş gauge (Figure 3a), the highest discharge period was observed from March to June (the highest value in April) and the lowest discharge period was from August to November (the lowest value in August). The annual mean discharge of the Gökırmak River is nearly stable during the instrumental period (Figure 3b). On the other hand, a slightly increasing trend is observed in the mean discharge of April–August (selected months for streamflow reconstruction—see below).

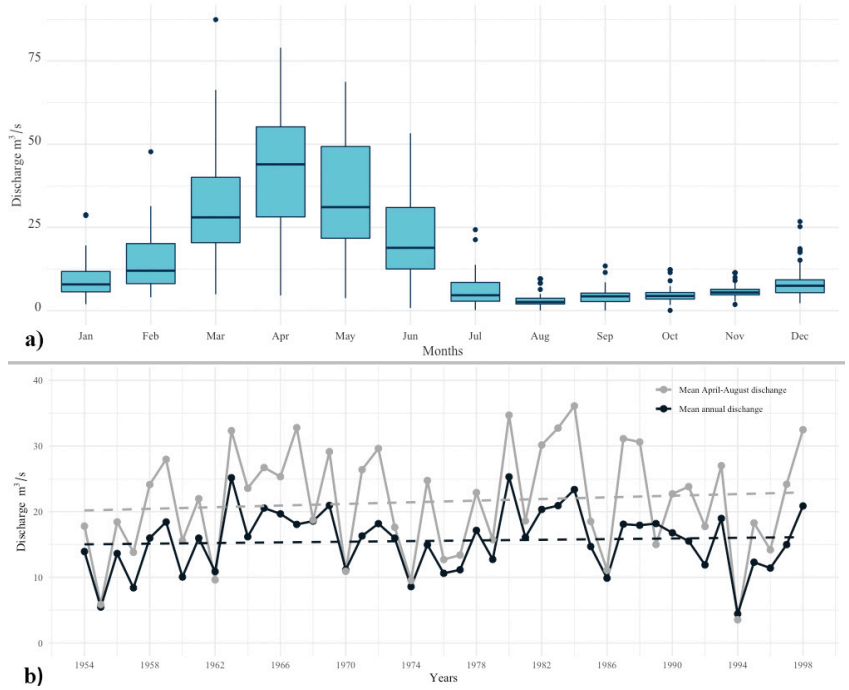

Figure 3. (**a**) The monthly hydrograph for Gökırmak River (at Kuyluş) gauge for the period of 1954–1998. The boxes of the boxplot representing half of the central data which start with the first quartile and end with the third quartile. Horizontal black line in the box represents the median. (**b**) The mean annual (black) and mean April–August (gray) discharge (m^3/s) with trend lines (dashed). The trend function is $y = -102 + 0.0624x$ for mean annual discharge and $y = -33.4 + 0.0248x$ for mean April–August discharge, where y indicates discharge and x indicates year.

2.4. Hydroclimate Reconstructions

Correlation coefficients were calculated to determine the relationships between climate (streamflow) and annual ring widths using the "*treeclim*" package in R [41,42]. Climate and streamflow data were considered as biological years, from previous October to current September [43]. The significance of the correlation coefficients was identified by bootstrapped confidence intervals. We obtained statistically significant correlations for April to July total precipitation ($P_{Apr–Jul}$) and April to August mean streamflow ($S_{Apr–Aug}$), which allowed us to reconstruct both precipitation and streamflow in the lower KRB.

The first step to obtain predictors of the reconstructions was the calculation of the principal components (PCs) of the seven chronologies. Then, PC_1 and PC_2 were selected by stepwise regression as predictors of the reconstructions. To reconstruct $P_{Apr-Jul}$, we applied a split-sample procedure [44], which divides instrumental time (1930–2003) into the two equal periods (1930–1967 and 1968–2003) for calibration and verification. We verified our calibration models by positive reduction in error (RE), and coefficient of efficiency (CE) values [43,45]. Then, our final reconstruction was calculated using the full period (1930–2003) for calibration.

Similarly, we also used the first two PCs for streamflow reconstruction. Our limitation for streamflow reconstruction was that the instrumental data is quite short (45 years long, 1954–1998) to apply a split-calibration method. We, therefore, used the whole period for calibration, then compared the results with precipitation reconstruction to verify it (e.g., [4]). The correlation coefficient between $P_{Apr–Jul}$ and $S_{Apr–Aug}$ was sufficiently high (0.67, $p < 0.01$) to verify our streamflow reconstruction with the precipitation reconstruction in the basin. The reconstructed values exceeding 1(2) standard deviation (SD) were identified as extreme dry/wet years and drought/flood events.

3. Results

3.1. Tree-Ring Data

We developed three climate-sensitive black pine chronologies from Sinop (HAC and MEM) and Çorum (BED) (Figure 4a, Table 2). The mean sensitivity values of the chronologies (HAC: 0.25, MEM: 0.27, and BED: 0.24) (Table 2) were found to be quite high, compared to the values in previous studies (0.13–0.27) from Turkey [4,20,22,23,46]. Newly developed chronologies of long-lived black pine forests (367, 242, 325 years long, respectively) with the drought-sensitive chronologies from previous studies (KAR, IKI, SAHand TIR) allowed us to build 210-year-long reconstructions dating back to 1794. High and significant correlation coefficients among the chronologies indicated common climate signals which account for much of the variability in the chronologies (Figure 4b).

The EPS value > 0.85 was reached in 1794 for MEM and BED chronologies and in 1698 for HAC chronology, and therefore, we applied the calibration equation for the period of 1794–2003 (Table 2).

3.2. Hydroclimate Reconstructions

We estimated missing monthly streamflow data of the Kuyluş gauge in the years 1954 (November and December), 1957 (May), 1961 (from January to November) and 1962 (December) using the monthly precipitation and temperature values. The Random Forest algorithm providing the highest correlation coefficient and the lowest error values were chosen among three algorithms (Simple Linear Regression, Bagging Regression, and Random Forest) of Weka machine learning software (Table 3).

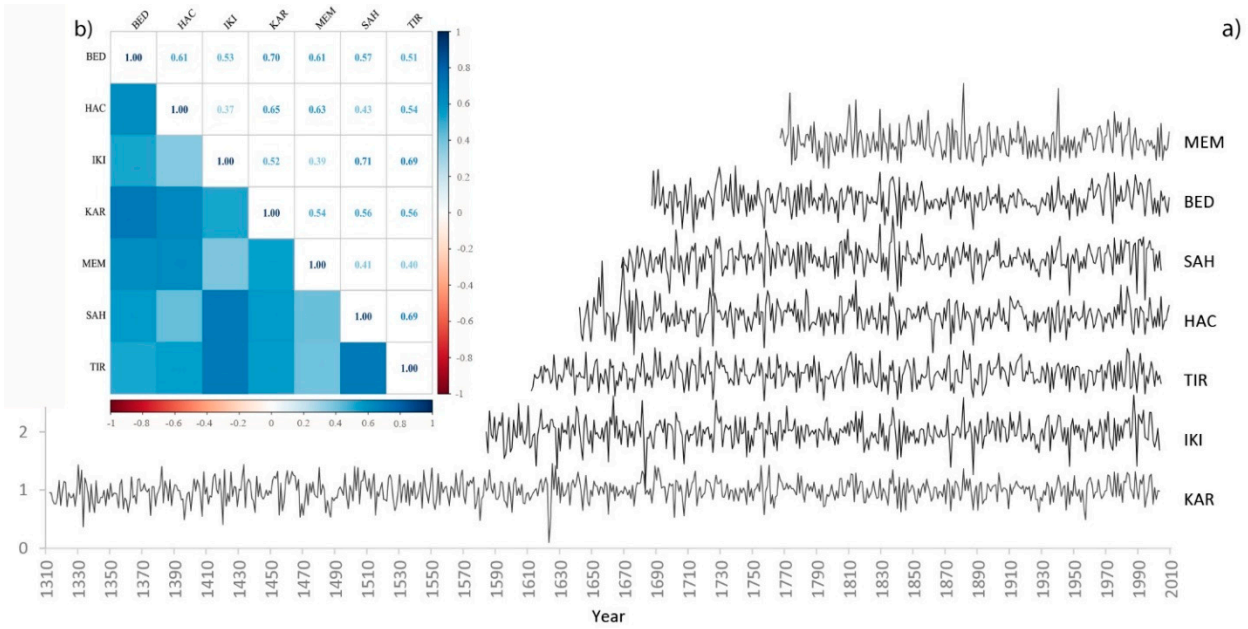

Figure 4. (**a**) The site chronologies and (**b**) correlation coefficients among each chronology for the period of 1794–2003. All correlation coefficients are significant ($p < 0.01$ for MEM and IKI, $p < 0.001$ for the remaining ones).

Table 2. Chronology statistics of the sites.

Sites	Chronology Time Span	Chronology Length	EPS > 0.85	MS	Mean Interseries Correlation	SNR
HAC	1642–2009	367	1689	0.25	0.68	10.3
MEM	1767–2009	242	1794	0.27	0.69	2.5
BED	1684–2009	325	1794	0.24	0.62	4.5

EPS: expressed population signal, MS: mean sensitivity, and SNR: signal-to-noise ratio.

Table 3. Calculated error values of algorithms used for machine learning.

	Simple Linear Regression					Bagging Regression					Random Forest				
MONTHS	Correlation Cofficient	Mean Absolute Error	Root Mean Square	Relative Absolute Error	Root Relative Squared Error	Correlation Cofficient	Mean Absolute Error	Root Mean Square	Relative Absolute Error	Root Relative Squared Error	Correlation Cofficient	Mean Absolute Error	Root Mean Square	Relative Absolute Error	Root Relative Squared Error
JAN	0.41	3.97	5.34	89.38%	91.28%	0.71	3.87	5.15	87.24%	88.01%	0.96	1.63	2.28	36.76%	38.99%
FEB	0.26	3.40	4.71	94.27%	96.45%	0.72	4.39	6.36	64.75%	73.58%	0.97	1.82	2.56	26.89%	29.67%
MAR	0.08	12.13	16.23	99.52%	99.68%	0.56	11.38	14.89	93.33%	91.46%	0.96	5.18	6.97	42.48%	42.80%
APR	0.59	13.17	15.56	82.34%	81.03%	0.80	10.37	12.00	64.89%	62.46%	0.97	4.22	5.39	26.39%	28.06%
MAY	0.25	13.45	15.98	97.81%	96.88%	0.67	9.95	12.55	72.35%	76.07%	0.96	4.47	5.63	32.50%	34.16%
JUN	0.40	8.94	11.73	86.45%	91.54%	0.67	8.22	10.40	79.49%	81.15%	0.95	3.70	4.94	35.75%	38.52%
JUL	0.26	3.40	4.71	94.27%	96.45%	0.51	3.15	4.49	87.33%	91.91%	0.94	1.53	1.98	42.42%	40.58%
AUG	0.41	1.70	2.35	88.95%	91.02%	0.64	1.60	2.20	83.79%	85.20%	0.97	0.65	0.87	34.02%	33.60%
SEP	0.07	1.81	2.55	98.67%	99.78%	0.65	1.58	2.25	86.24%	88.19%	0.97	0.69	0.95	37.49%	37.38%
OCT	0.25	1.68	2.42	98.74%	96.87%	0.59	1.49	2.12	87.61%	85.10%	0.93	0.82	1.10	48.35%	44.17%
NOV	0.06	1.78	2.37	99.43%	99.81%	0.42	1.69	2.26	94.07%	94.81%	0.96	0.80	0.97	44.62%	40.96%
DEC	0.17	4.12	5.58	95.74%	98.52%	0.42	3.65	5.15	84.76%	90.93%	0.94	1.85	2.51	43.05%	44.30%

The correlation coefficients between the site chronologies and climate (streamflow) (Figure 5) showed that drought, associated with negative correlation coefficients of temper-

ature and positive and significant correlations of precipitation during mid-spring-summer, has dominant control of tree-ring formation. The effect of precipitation was stronger than temperature. The highest and significant correlations are calculated with precipitation from April to July and with streamflow from April to August, which indicate the months taken into account in the reconstructions.

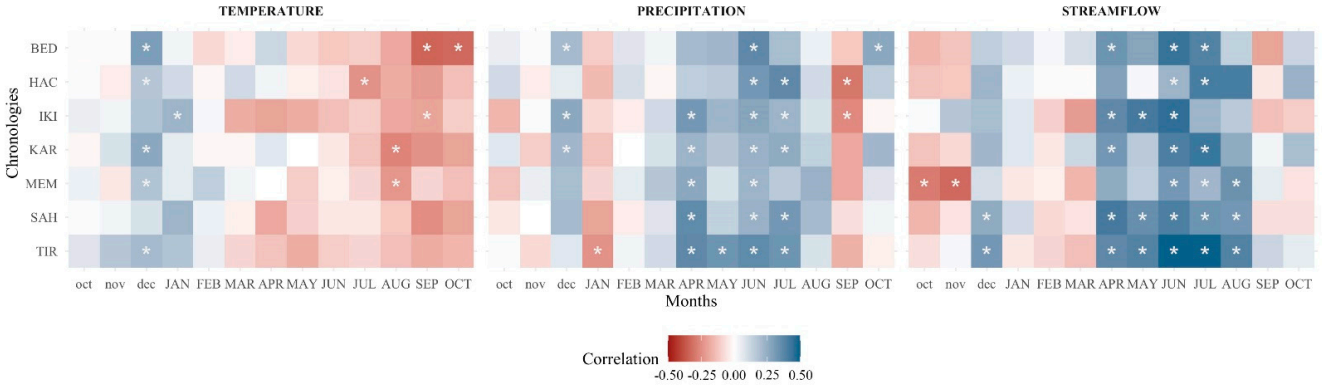

Figure 5. The correlation coefficients of climate variables with the tree-ring formations between 1930–2003 (except TIR, 1930–2000). Asterisk symbols represent the statistically significant months.

We used PC_1 and PC_2 as predictors, which explain 66% of the total variance, in the following equation to reconstruct April to July total precipitation:

$$P_{April–July} = 31.67 + 65.38PC_1 - 16.69PC_2$$

The split-sample procedure provided significant calibration and verification statistics, represented by positive RE and CE values as well as significant F values, for both calibration periods (Table 4). Then, we used precipitation data of the full period (1930–2003) for the final reconstruction (Figure 6), explaining 36% of instrumental precipitation data variance. In this research, we developed 210-year-long spring–summer precipitation reconstruction for lower KRB (Figure 7).

Table 4. Calibration and verification statistics of $P_{April–July}$ and $S_{April–August}$ reconstructions.

	Calibration Period	Verification Period	R^2	Adj. R^2	F	RE	CE
Precipitation	1930–1967	1968–2003	0.38	0.34	10.56 $p < 0.001$	0.35	0.35
	1968–2003	1930–1967	0.33	0.29	8.47 $p < 0.001$	0.33	0.33
	1930–2003	-	0.36	0.33	19.6 $p < 0.001$	-	-
Streamflow	1954–1998	-	0.35	0.32	11.3 $p < 0.001$	-	-

We were only able to use the full period (1954–1998) in calibration to reconstruct April–August streamflow data of Gökırmak due to instrumental record being too short to be applied using a split-sample procedure:

$$S_{April–August} = -4.745 + 9.926PC_1 - 8.345PC_2$$

The reconstruction successfully explained 35% of the variance in the instrumental data. Visual and statistical agreement between two reconstructions (Figure 6, Table 3) verified our $S_{April–August}$ reconstruction.

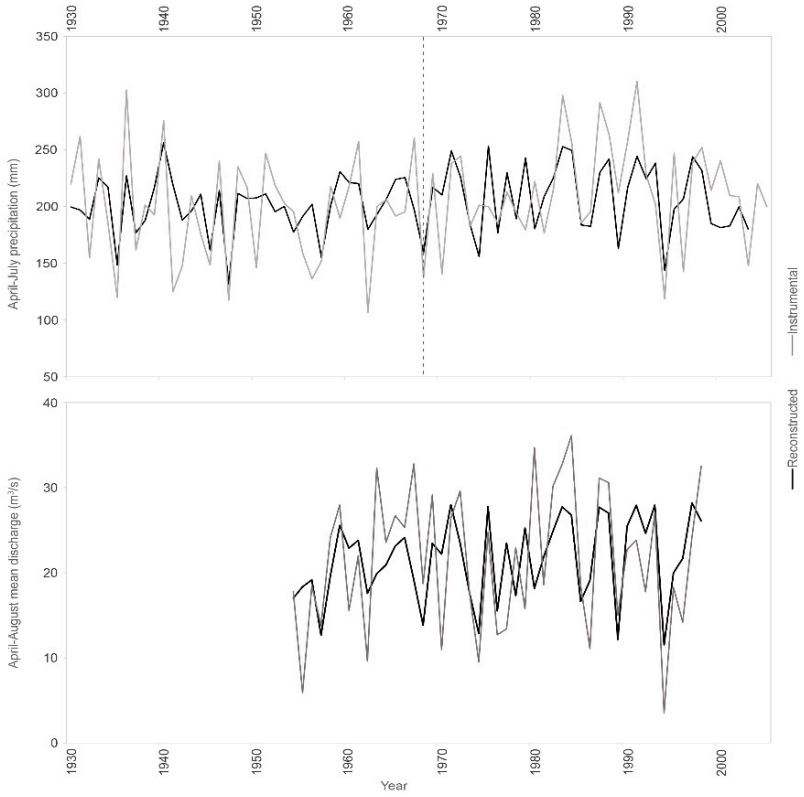

Figure 6. Instrumental and reconstructed April-July total precipitation (mm) (upper) and instrumental and reconstructed mean April–August Gökırmak River streamflow (m^3/s) (lower). Vertical gray dashed line indicates split calibration and verification periods of precipitation reconstruction.

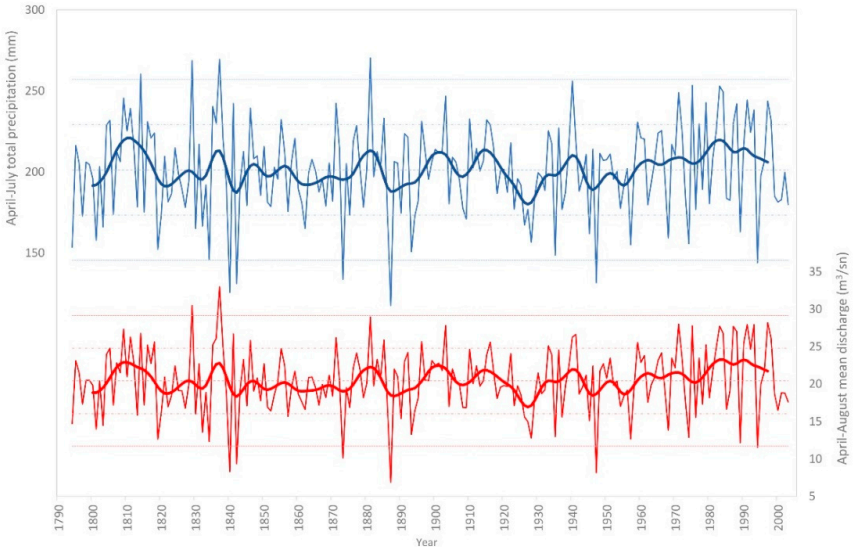

Figure 7. April–July total precipitation (mm) reconstruction of the lower KRB (blue line, upper) and April–August mean Gökırmak River streamflow (m^3/s) reconstruction (red line, lower). The dashed blue (red) central, inner and outer horizontal lines indicate the mean of estimated values and the border of 1(2) SDs from the mean, respectively, and the solid red (blue) line shows the 13-year low-pass filter value.

The dry (drought) and wet (flood) years in the $P_{April–July}$ ($S_{April–August}$) reconstruction are presented for the pre-instrumental period (here, we listed the years before 1954 when the gauge records started; even the meteorological records exist after 1930) in Table 5. We

listed 22 drought (−1SD) and 20 flood (+1SD) events for the $S_{April–August}$ reconstruction. Five more dry years (1797, 1820, 1862, 1894 and 1909) and four more wet years (1805, 1855, 1910, and 1915) were determined for $P_{April–July}$, in addition to $S_{April–August}$. Extreme drought (1840, 1842, 1873, 1887, and 1947) and flood events (1829 and 1837) of $S_{April–July}$ were the same as extreme dry and wet events of $P_{April–July}$.

Table 5. The dry/drought and wet/flood years of $P_{April-July}$/$S_{April–August}$ reconstructions.

	18th Century	19th Century		20th Century
	1750–1799	**1800–1849**	**1850–1899**	**1900–1949**
Dry events	1794 [20,23,47] 1797 [17,18,20,48,49]	1801 [20] 1803 1813 [47,50] 1819 [21] 1820 [20,49,51] 1830 [20,47] 1832 [20,21,23,47] 1834 [4,20,47,50,51] **1840** [4,20,21,23,47–52] **1842** [4,18]	1857 1862 **1873** [10,21,23,47,53–58] **1887** [4,10,21,23,47–49,51,52,55,57–61] 1890 [20,47,49–51,59,60,62] 1893 [4,20,21,47–49,51,59,63] 1894 [20,21]	1909 [20,21,47–49] 1926 [18,20,47,52,58,64] 1927 [4,18,20,23,47–49,51,52,58,59,64] 1928 [4,18,20,21,23,47–49,51,52,58–61,64,65] 1935 [18,21,49–51,60] 1937 1945 [18,23,60] **1947** [20,58]
Wet events	-	1805 1809 [20,21,49,51] 1811 [4,17,20,21,47,59] ***1814*** [4,23] 1816 [4,17,20,21,47,50,51,59] 1818 [20,23,49] **1829** [4,20,23,48,50] 1835 [20,21,47] 1836 [20,21] **1837** [4,20] 1841 [20,47,48] 1846 [20,21,23,47,48,50]	1855 [20,21,60] 1871 [4,48,59] ***1881*** [4,17,20,47,48,50,59,60] 1885 [4,20,47–49,51] 1896 [51,59,60]	1903 [4,50] 1910 [17,18,20,54,59] 1915 [20,21] 1916 1933 [60] 1940 1941 [50]

Events observed only precipitation reconstruction; and **bold** and *italic* fonts indicate extreme wet years observed only precipitation reconstruction. The **bold** fonts indicate the extreme dry and wet events; underlined fonts indicate dry and wet.

Additively, $P_{April–July}$ has two more extreme wet years (1814 and 1881), which are flood events in $S_{April–July}$. The driest year in both reconstructions was 1887, while the wettest year was 1881 in $P_{April–July}$ and the highest flow was 1837 in the $S_{April–July}$ reconstruction.

The dry (drought) and wet (flood) years were generally one-year-long. The longest consecutive drought was three years long and was observed between the years 1926 and 1928. Two year-long dry events (1819–1820 and 1893–1894) were determined only for the $P_{April–July}$ reconstruction. Similarly, the longest consecutive wet (flood) period was three years long from 1835 to 1837. The two year-long wet events were 1915–1916 (for only $P_{April–June}$ reconstruction) and 1940–1941 (for both).

4. Discussion

In this research, we provided precipitation and streamflow reconstructions for the lower KRB going back to 1794. The streamflow reconstruction is one month longer (April to August) than the precipitation reconstruction (April to July). Similarly, Güner et al. (2017) [23] reported a one-month lag between precipitation and streamflow in Sakarya Basin. Both reconstructions largely overlapped in terms of dry (drought) and wet (flood) events as well as long-term variability (13-year filtering). This is because the flow in the KRB takes its source from rain and snow waters, which are generally correlated with precipitation in the basin [26]. The synchronization is an additional verification for our streamflow calibration equation.

Historical dry and wet years, as well as drought and flood events in lower KRB, were highly coincident with previous reconstructions and historical documents (Table 5). For instance, the driest year of the lower KRB, the year of 1887 (118 mm total $P_{April–June}$ and 6.9 m^3/s mean $S_{April–August}$), was also mentioned as the driest year during the last

215-year-long period for Western Anatolia [20], which is adjacent to the western border of our research area. Moreover, low flows were determined for Filyos [4] and Sakarya [23] rivers this year. Severe drought, mostly due to low snowfall in winter and unfavorable weather conditions until May [57], caused a major famine in the whole Ottoman Empire lands [66] in 1887.

We were unable to reach a historical document for 1840 and 1842, which were the extreme dry years of the lower KRB. In addition, both years (mostly 1840) were determined to be dry years by the previous reconstructions in Turkey (Table 5). Köse et al. (2011) [20] listed 1840 as one of the exceptionally dry years (1794, 1840, 1887, and 1893) of the last two centuries covering all western Anatolia.

The extreme drought was observed in our reconstruction in 1873, with 134 mm $P_{April–June}$ and 10.1 m^3/s mean $S_{April–August}$. The Ottoman Archives reported that thousands of people and animals died in Anatolia due to severe drought and famine occurring in the consecutive two years from 1873 to 1874 [53,56,67,68]. Central Anatolia, including lower KRB, faced a catastrophic famine in 1873, and warehouses were plundered by the people [55]. This year is listed as one of the extreme dry or dry years by almost all previous reconstructions in Anatolia (Table 5).

The last extreme drought determined by our research was in April–July (August) of 1947. Brazdil et al. (2016) [69] stated that the April-October period of this year was very hot and dry for the area, from the Iberian Peninsula and extending through Central Europe to Turkey. Moreover, 1947–1950 is counted among the dry periods that have caused great damage to the economy of Turkey during the last 60 years [70]. This period appears as a drought period represented by 13-year filters of both reconstructions (Figure 7).

In our reconstruction, 1893 was determined as a dry year, coinciding with most of the previous reconstructions (Table 5). The Ottoman Archives reported a three-year-long consecutive drought between 1891 and 1893 due to insufficient precipitation, which particularly affected Eastern Anatolia and was also seen in the inner parts of the Black Sea Region and Tripoli [63].

The duration of the dry and wet years obtained from our reconstructions showed similar patterns to previous precipitation reconstructions from Turkey [4,18,20,21,23]. The longest consecutive wet years (1835–1837) observed in the lower KRB were also determined for Western Anatolia by Köse et al. (2011) [20]. Moreover, the longest consecutive dry years (1926–1928) of the lower KRB almost overlapped with the four-year-long drought (1925–1928) observed in Anatolia [64] and was determined by the reconstructions [20]. Most of the extreme dry years of our reconstruction were verified by famine and drought events in the historical documents mentioned above. On the other hand, wet (flood) years could not be compared with the documents, because the archives record mostly catastrophic events [20]. Wet (flood) events highly correlated with previous reconstructions (Table 5).

The long-term variability represented by the 13-year low-pass filters of reconstructed $P_{April–July}$ and $S_{April–August}$ was largely coherent, except for after 1985 (Figure 7). Güner et al. (2017) [23] stated a sharp decline in the June–July discharge of the Kocasu River in Sakarya Basin after the 1960s. Conversely, our $S_{April–August}$ reconstruction showed a slight increase. This increasing trend is also observed on the instrumental mean April–August discharge records of the Gökırmak River (Figure 3b). The low-pass filtering values of the $S_{April–August}$ reconstruction were stable, with the values close to mean during the period of 1843–1872, while consequent dry and wet periods occured before and after this 30-year period. A similar stationary pattern was also found in Fernández et al. (2018) [14].

5. Conclusions

In this research, we added three new drought-sensitive black pine chronologies to the tree-ring network of Turkey, which are suitable to use for further tree-ring studies. In addition, we provided 210-year-long spring–summer precipitation and streamflow reconstructions for the lower KRB. The extreme droughts observed in our reconstructions demonstrated high coincidence with the catastrophic events in historical documents. Know-

ing that the longest consecutive drought was three years long during the last two centuries indicates that the basin may experience similar or longer droughts in the future. Multi-century reconstructions constitute an important basis for planning the future of water resources, especially in regions such as the Mediterranean Basin, where the negative effects of climate change are detected in natural resources. In conclusion, our results provide a reliable source to help prepare for the worst-case scenarios of climate change in one of the most strategically important rivers of Turkey.

Author Contributions: H.T.G. collected tree ring samples; S.G. performed tree-ring measurements; S.G. and H.T.G. performed dendrochronological analysis and dendrohydrological reconstructions; Figures were created by S.G. and H.T.G.; H.T.G. wrote the paper. All authors have read and agreed to the published version of the manuscript.

Funding: This research received no external funding.

Data Availability Statement: The data presented in this study are available on request from the corresponding author.

Acknowledgments: We are grateful to Nesibe Köse, Ünal Akkemik, and H. Nüzhet Dalfes for sharing their tree-ring data and encouraging us to build streamflow reconstruction in the lower Kızılırmak Basin. Coşkun Köse and Ali Kaya are thanked for helping us in the field. Special thanks to the staff of the Sinop Regional Directorate of Forestry and Kargı Forest District Directorate for various kinds of help during our field work. Evrim Ayşe Şahan helped improve the final manuscript.

Conflicts of Interest: The authors declare no conflict of interest.

References

1. Bègin, Y. Reconstruction of Subarctic Lake Levels Over Past Centuries using Tree Rings. *J. Cold Reg. Eng.* **2000**, *14*, 192–212. [CrossRef]
2. Chen, F.; Shang, H.; Panyushkina, I.; Meko, D.; Li, J.; Yuan, Y.; Yu, S.; Chen, F.; He, D.; Luo, X. 500-year tree-ring reconstruction of Salween River streamflow related to the history of water supply in Southeast Asia. *Clim. Dyn.* **2019**, *53*, 6595–6607. [CrossRef]
3. Jones, P.D.; Briffa, K.; Pilcher, J.R. Riverflow reconstruction from Tree Rings in Southern Britain. *J. Clim.* **1984**, *4*, 461–472. [CrossRef]
4. Akkemik, Ü.; D'Arrigo, R.; Cherubini, P.; Köse, N.; Jacoby, G.C. Tree-ring reconstructions of precipitation and streamflow for north-western Turkey. *Int. J. Clim.* **2008**, *28*, 173–193. [CrossRef]
5. Anderson, S.R.; Ogle, R.; Tootle, G.; Oubeidillah, A. Tree-Ring Reconstructions of Streamflow for the Tennessee Valley. *Hydrology* **2019**, *6*, 34. [CrossRef]
6. Case, R.A.; MacDonald, G.M. Tree ring reconstruction of Streamflow for Three Canadian Prairie Rivers. *J. Am. Water Resour. Assoc.* **2003**, *39*, 703–716. [CrossRef]
7. Wise, E.K. Tree ring record of streamflow and drought in the upper Snake River. *Water Resour. Res.* **2010**, *46*, W11529. [CrossRef]
8. Cook, E.R.; Seager, R.; Kushnir, Y.; Briffa, K.R.; Büntgen, U.; Frank, D.; Krusic, P.J.; Tegel, W.; van der Schrier, G.; Andreu-Hayles, L.; et al. Old World megadroughts and pluvials during the Common Era. *Sci. Adv.* **2015**, *1*, e1500561. [CrossRef]
9. Ewane, B.E.; Lee, H.H. Tree-ring reconstruction of streamflow for Palgong Mountain forested watershed in southeastern South Korea. *J. Mt. Sci.* **2017**, *14*, 60–76. [CrossRef]
10. Stagge, J.H.; Rosenberg, D.E.; DeRose, R.J.; Rittenour, T.M. Monthly paleostreamflow reconstruction from annual tree-ring chronologies. *J. Hydrol.* **2018**, *557*, 791–804. [CrossRef]
11. Meko, D.M.; Therrell, M.D.; Baisan, C.H.; Hughes, M.K. Sacramento River Flow Reconstructed to A.D. 869 From Tree Rings. *J. Am. Water Resour. Assoc.* **2001**, *37*, 1029–1039. [CrossRef]
12. Woodhouse, C.A.; Lukas, F.J. Multi-Century Tree-ring Reconstructions of Colorado Streamflow Water Resource Planning. *Clim. Chang.* **2006**, *78*, 293–315. [CrossRef]
13. Touchan, R.; Woodhouse, C.A.; Meko, D.M.; Allen, C. Millennial precipitation reconstruction for the Jemez Mountains, New Mexico, reveals changing drought signal. *Int. J. Clim.* **2011**, *31*, 896–906. [CrossRef]
14. Fernández, A.; Muñoz, A.; González-Reyes, Á.; Aguilera-Betti, I.; Toledo, I.; Puchi, P.; Sauchyn, D.; Crespo, S.; Frene, C.; Mundo, I.; et al. Dendrohydrology and Water Resources Management in South-Central Chile: Lessons from the Río Imperial Streamflow Reconstruction. *Hydrol. Earth Syst. Sci.* **2018**, *22*, 2921–2935. [CrossRef]
15. Ballesteros-Canovas, J.A.; Bombino, G.; D'Agostinoa, D.; Denisia, P.; Labatea, A.; Stoffel, M.; Zemaa, D.A.; Zimbonea, S.M. Tree-ring based, regional-scale reconstruction of flash floods in Mediterranean mountain torrents. *Catena* **2019**, *189*, 104481. [CrossRef]

16. Jansma, E. Hydrological disasters in the NW-European Lowlands during the first millennium AD: A dendrochronological reconstruction. *Neth. J. Geosci.* **2020**, *99*, E11. [CrossRef]
17. Akkemik, Ü.; Dagdeviren, N.; Aras, A. A preliminary reconstruction (AD 1635-2000) of spring precipitation using oak tree rings in the western Black Sea region of Turkey. *Int. J. Biometeorol.* **2005**, *49*, 297–302. [CrossRef]
18. Touchan, R.; Xoplaki, E.; Funchouser, G.; Luterbacher, J.; Hughes, M.K.; Erkan, N.; Akkemik, Ü.; Stephan, J. Reconstruction of spring/summer precipitation for the Eastern Mediterranean from tree-ring widths and its connection to large–scale atmospheric circulation. *Clim. Dyn.* **2005**, *25*, 75–98. [CrossRef]
19. Touchan, R.; Akkemik, Ü.; Huges, M.K.; Erkan, N. May–June precipitation reconstruction of southwestern Anatolia, Turkey during the last 900 years from tree-rings. *Quat. Res.* **2007**, *68*, 196–202. [CrossRef]
20. Köse, N.; Akkemik, Ü.; Dalfes, H.N.; Özeren, M.S. Tree-ring reconstructions of May–June precipitation of western Anatolia. *Quat. Res.* **2011**, *75*, 438–450. [CrossRef]
21. Köse, N.; Akkemik, Ü.; Güner, H.T.; Dalfes, H.N.; Grissino-Mayer, H.D.; Özeren, M.S.; Kındap, T. An improved reconstruction of May–June precipitation using tree-ring data from western Turkey and its links to volcanic eruptions. *Int. J. Biometeorol.* **2013**, *57*, 691–701. [CrossRef] [PubMed]
22. Köse, N.; Güner, H.T.; Harley, G.L.; Guiot, J. Spring temperature variability over Turkey since 1800 CE reconstructed from a broad network of tree-ring data. *Clim. Past.* **2017**, *13*, 1–15. [CrossRef]
23. Güner, H.T.; Köse, N.; Harley, G.L. A 200-year reconstruction of Kocasu River (Sakarya River Basin, Turkey) streamflow derived from a tree-ring network. *Int. J. Biometeorol.* **2017**, *61*, 427–437. [CrossRef] [PubMed]
24. Çakmak, B. Kızılırmak Havzası Sulama Birliklerinde Sulama Sistem Performansının Değerlendirilmesi. *KSÜ Fen Ve Mühendislik Derg.* **2002**, *5*, 130–141.
25. Marmara Research Center (MAM), Tübitak. Havza Koruma Eylem Planlarının Hazırlanması-Kızılırmak Havzası. Turkish Ministry of Agriculture and Forestry, General Directorate of Water Management 2010. Available online: https://www.tarimorman.gov.tr/SYGM/Belgeler/havza%20koruma%20eylem%20planlar%C4%B1/K%C4%B1z%C4%B1l%C4%B1rmak_Havzas%C4%B1.pdf (accessed on 2 February 2022).
26. Efe, R. Kızılırmağın Akım ve Rejim Özellikleri. *Marmara Üniversitesi Sos. Bilimler Enstitüsü Derg.* **1996**, *3*, 39–60.
27. Yüce, M.İ.; Ercan, B. Kızılırmak Havzası Yağış Akış ilişkisinin Belirlenmesi. In Proceedings of the 4. Su Yapıları Sempozyumu, Antalya, Turkey, 19–21 November 2015; pp. 410–418.
28. Hızal, A.; Serengil, Y.; Özcan, M. Ekosistem Tabanlı Havza Planlama Metodolojisi ve Havza Çalışmalarında Yapılan Yanlış Uygulamalar. In Proceedings of the TMMOB 2. Su Politikaları Kongresi, Ankara, Türkiye, 20–22 March 2008; pp. 1–12.
29. Mayer, H.; Aksoy, H. *Türkiye Ormanları*; Batı Karadeniz Ormancılık Araştırma Enstitüsü Müdürlüğü, Abant İzzet Baysal Üniversitesi Basımevi: Bolu, Turkey, 1998; p. 291.
30. Stokes, M.A.; Smiley, T.L. *An Introduction to Tree-ring Dating*, 2nd ed.; The University of Arizona Press: Tucson, AZ, USA, 1996; pp. 1–73. ISBN 978-0816516803.
31. Speer, J.H. *Fundamentals of Tree-Ring Research*; University of Arizona Press: Tucson, AZ, USA, 2010; ISBN 978-0816526857.
32. Holmes, R.L. Computer-assisted quality control in tree-ring data and measurements. *Tree-Ring Bull.* **1983**, *43*, 69–78.
33. Grissino-Mayer, H.D. Research Report Evaluating Crossdating Accuracy: A Manual and Tutorial for the Computer Program Cofecha. *Tree-Ring Res.* **2001**, *57*, 205–221.
34. Cook, E.R. A Time Series Analysis Approach to Tree-Ring Standardization. Ph.D. Thesis, University of Arizona, Tucson, AZ, USA, 1985.
35. Cook, E.R.; Shiyatov, S.; Mazepa, M. Estimation of the mean chronology. In *Methods of Dendrochronology: Applications in the Environmental Sciences*; Cook, E., Kairiukstis, L., Eds.; Kluwer Academic Publishers: Dordrecht, The Netherlands, 1990; pp. 123–132, ISBN 978-90-481-4060-2. Available online: http://pure.iiasa.ac.at/id/eprint/3354/1/Methods_of_Dendrochronology_Applications.pdf (accessed on 7 February 2022).
36. Biondi, E.; Swetnam, T.W. Box-Jenkins models of forest interior tree-ring chronologies. *Tree-Ring Bull.* **1987**, *47*, 71–95.
37. Wigley, T.M.L.; Briffa, K.R.; Jones, P.D. On the average value of correlated time series, with applications in dendroclimatology and hydrometeorology. *J. Appl. Meteorol. Climatol.* **1984**, *23*, 201–213. [CrossRef]
38. Briffa, K.; Jones, P.D. Basic chronology statistics and assessment. In *Methods of Dendrochronology: Applications in The Environmental Sciences*; Cook, E., Kairiukstis, L., Eds.; Kluwer Academic Publishers: Dordrecht, The Netherlands, 1990; pp. 137–152. ISBN 978-90-481-4060-2.
39. Harris, I.; Osborn, T.; Jones, P.; Lister, D. Version 4 of the CRU TS monthly high-resolution gridded multivariate climate dataset. *Sci. Data* **2020**, *7*, 109. [CrossRef]
40. Witten, I.H.; Frank, E.; Hall, M.A. The WEKA Data Mining Workbench. In *Data Mining: Practical Machine Learning Tools and Techniques*, 4th ed.; Witten, I.H., Frank, E., Hall, M.A., Pal, C.J., Eds.; Morgan Kaufmann: Burlington, MA, USA, 2017; pp. 553–571, ISBN 978-0128042915.
41. R Development Core Team. *R: A Language and Environment for Statistical Computing*; R Foundation for Statistical Computing: Vienna, Austria, 2009.
42. Zang, C.; Biondi, F. Treeclim: An R package for the numerical calibration of proxy-climate relationships. *Ecography* **2015**, *38*, 431–436. [CrossRef]
43. Fritts, H.C. *Tree Rings and Climate*; Academic Press: London, UK, 1976; pp. 1–567, ISBN 978-0-12-268450-0.

44. Meko, D.M.; Graybill, D.A. Tree-ring reconstruction of upper Gila River discharge. *Water Res. Bull.* **1995**, *31*, 605–616. [CrossRef]
45. Cook, E.R.; Briffa, K.R.; Jones, P.D. Spatial regression methods in dendroclimatology: A review and comparison of two techniques. *Int. J. Clim.* **1994**, *14*, 379–402. [CrossRef]
46. Doğan, M.; Köse, N. Four new tree-ring chronologies from old black pine forests of Sandıras Mountain (Mugla, Turkey). *J. Fac. For. Istanb. Univ.* **2015**, *65*, 1–16. [CrossRef]
47. Köse, N.; Akkemik, Ü.; Dalfes, H.N. Anadolu'nun iklim tarihinin son 500 yılı: Dendroklimatolojik ilk sonuçlar. In Proceedings of the Türkiye Kuvaterner Sempozyumu-TURQUA–V, Istanbul, Türkiye, 2–3 June 2005; pp. 136–142.
48. Akkemik, Ü.; Cherubini, P. *Batı Karadeniz Bölgesi'nde Doğal Yetişen Gymnosperm Taksonları Üzerinde Dendrokronolojik Araştırmalar*; Project TÜBİTAK TOGTAG-2703; TÜBİTAK: Ankara, Türkiye, 2003. (In Turkish)
49. Akkemik, Ü.; Aras, A. Reconstruction (1689–1994) of April-August precipitation in southwestern part of central Turkey. *Int. J. Clim.* **2005**, *25*, 537–548. [CrossRef]
50. Martín-Benito, D.; Ummenhofer, C.; Köse, N.; Güner, H.T.; Pederson, N. Tree-ring reconstructed May–June precipitation in the Caucasus since 1752 CE. *Clim. Dyn.* **2016**, *47*, 3011–3027. [CrossRef]
51. Touchan, R.; Garfin, G.M.; Meko, D.M.; Funchouser, G.; Erkan, N.; Hughes, M.K.; Wallin, B.S. Preliminary reconstruction of spring precipitation in southwestern Turkey from tree ring width. *Int. J. Clim.* **2003**, *23*, 157–171. [CrossRef]
52. Touchan, R.; Funkhouser, G.; Hughes, M.K.; Erkan, N. Standardized precipitation index reconstructed from Turkish ring widths. *Clim. Chang.* **2005**, *72*, 339–353. [CrossRef]
53. Quataert, D. Famine in Turkey—1873–1875. Master's Thesis, Binghamton University, New York, NY, USA, 1968.
54. Newton, M.W.; Kuniholm, P.I. Wiggles Worth Watching Making Radiocarbon Work. In *The Case of Çatal Höyük Studies in Aegean archaeology presented to Malcolm H. Wiener as he enters his 65th year, Meleemata*; Betancourt, P.P., Karageorghis, V., Laffineur, R., Niemeir, W.D., Eds.; Université de Liège, Histoire de l'art et Archéologie de la Grèce Antique: Austin, TX, USA, 1999; pp. 1–968, ISBN 978-1935488149.
55. Aybar, M. Osmanlı Devletinde Kıtlık ve İç Göç: 1870-1900 Arası İç Anadolu Örneği. *Mavi. Atlas.* **2017**, *5*, 474–488. [CrossRef]
56. Bayar, Y. *1873–1875 Orta Anadolu Kıtlığı*; Yüksek Lisans Tezi, Marmara Üniversitesi Türkiyat Araştırmaları Enstitüsü: Istanbul, Turkey, 2013.
57. Altındaş, E.T. 19. yüzyılda Osmanlı Devleti'nde Yaşanan Kuraklığın Ankara'ya Yansıması. *Çanakkale Araştırmaları Türk Yıllığı* **2018**, *16*, 1–13. [CrossRef]
58. Ottoman Archives (1850–1923) Documents (correspondence between Ottoman Palace and provinces) in the Directory of State Archives of Prime Ministry of Republic of Turkey. Unpublished work.
59. D'Arrigo, R.; Cullen, H.M. A 350-year (AD 1628-1980) reconstruction of Turkish precipitation. *Dendrochronologia* **2001**, *19*, 169–177.
60. Hughes, M.K.; Kuniholm, P.I.; Garfin, G.M.; Latini, C.; Eischeid, J.K. Aegean tree-ring signature years explained. *Tree-Ring Res.* **2001**, *57*, 67–73.
61. Purgstal, B.J.V.H. *Osmanlı Devleti Tarihi, Cilt.1-7*; Bürün, V., Translator; Üçdal Publishing: Istanbul, Turkey, 1983.
62. Afkhami, A. Disease and water supply: The case of cholera in 19th century Iran. In *Transformations of Middle Eastern Natural Environments: Legacies and Lessons*; Coppock, J., Miller, J., Eds.; Yale University: New Haven, CT, USA, 1998; Volume 103, pp. 206–220.
63. Özger, Y. XIX. yüzyıl sonlarında meydana gelen bir kuraklık ve kıtlık hadisesi ile bunun sosyo–ekonomik sonuçları. *Karadeniz Araşt* **2008**, *19*, 87–96.
64. Kadıoğlu, M. *Bildiğiniz Havaların Sonu-Küresel İklim Değişimi ve Türkiye*; Güncel Yayınları: İstanbul, Turkey, 2001; ISBN 9786058017887.
65. Inalcik, H. A Note on the Population of Cyprus. 1997. Available online: http://sam.gov.tr/pdf/perceptions/Volume-II/june-august-1997/HalilInalcik2.pdf (accessed on 3 February 2022).
66. Gül, A. Drought and famine in Ottoman Empire (Case of Erzurum Province: 1892–1893 and 1906–1908). *J. Int. Soc. Res.* **2009**, *2*, 144–158.
67. Davison, H.R. *Reform in the Ottoman Empire*; Princeton University Press: Princeton, NJ, USA, 1963; pp. 1–494. ISBN 9780691651644.
68. Faroqhi, S. *The Ottoman Empire: A Short History*; Frisch, S., Translator; Markus Wiener Publishers: Princeton, NJ, USA, 2009; ISBN 978-1558764491.
69. Brazdil, R.; Raška, P.; Trnka, M.; Zahradníček, P.; Valasek, H.; Dobrovolny, P.; Řezníčková, L.; Treml, P.; Stachoň, Z. The Central European drought of 1947: Causes and consequences, with particular reference to the Czech Lands. *Clim. Res.* **2016**, *70*, 161–178. [CrossRef]
70. Çiçek, İ. Türkiye'de Kurak Dönemin Yayılışı ve Süresi (Homethwaite Metoduna Göre). *Türkiye Coğrafyası Araştırma Uygul. Merk. Derg.* **1993**, *4*, 77–101.